Research Article

Antibacterial Additive for Polystyrene Based on Silver Nanoparticles Supported on Titanium Dioxide

Miguel A. Waldo-Mendoza,[1,2] Lucía Martínez-Jothar,[3] Socorro Oros-Ruiz,[4] E. G. Villabona-Leal,[3] Luis Manuel Céspedes-Covarrubias,[2] Zoe V. Quiñones-Jurado,[2] Eduardo Ortega,[5] and Elías Pérez[3]

[1]*Facultad de Ciencias Químicas, Universidad Autónoma de San Luis Potosí, Av. Manuel Nava No. 6, Zona Universitaria, 78290 San Luis Potosí, SLP, Mexico*
[2]*Innovación y Desarrollo en Materiales Avanzados, A.C., Grupo Polynnova, Carretera San Luis Potosí-Guadalajara No. 1510, Nivel 3, Despacho 13, Fraccionamiento Lomas del Tecnológico, 78211 San Luis Potosí, SLP, Mexico*
[3]*Instituto de Física, Universidad Autónoma de San Luis Potosí, Álvaro Obregón 64, 78000 San Luis Potosí, SLP, Mexico*
[4]*Departamento de Química, Universidad Autónoma Metropolitana-Iztapalapa, 09340 Ciudad de México, Mexico*
[5]*Departamento de Física, Tecnológico de Monterrey, 64849 Monterrey, NL, Mexico*

Correspondence should be addressed to Elías Pérez; elias@ifisica.uaslp.mx

Silver nanoparticles supported on titanium dioxide nanoparticles (Ag/TiO_2) were incorporated and evaluated as antibacterial additive for polystyrene materials. These particles were synthesized using a deposition-precipitation method by adding silver nitrate as metallic precursor, sodium hydroxide as reducing agent, and commercial TiO_2 (P25) as support. Rectangular pieces of polystyrene (PS) containing 100, 300, 500, and 700 ppm (wt.%) of the additive were made using an extrusion-injection molding process, and they were evaluated for their antibacterial properties against *Escherichia coli* using the Pour Plate method. Particles were distributed on the PS surface, and PS pieces presented a good antibacterial efficiency at 100, 300, and 500 ppm and decreased for 700 ppm due to an additive agglomeration on the PS surface. These results validate the antibacterial properties of Ag/TiO_2, determine a concentration limit at which the additive is well distributed on the PS surface, and assess the importance of Ag in this system.

1. Introduction

Antimicrobials are natural or synthetic chemical compounds that kill or suppress the growth of viruses, bacteria, and/or fungi. Activity against bacteria and fungi is currently of major interest in the plastic industry as it promotes preservation and increased shelf life of the goods [1]. Polystyrene is an easily moldable material for injection, blown, extrusion, and thermoformed processes. It is also a material with wide applications in electrodomestics and food and pharmaceutical containers. These applications made polystyrene a suitable material to test the Ag/TiO_2 composite as an antimicrobial agent [2].

The use of silver based antimicrobials has dramatically increased in the plastic industry due mainly to low toxicity to humans as well as long-lasting efficacy. Silver (Ag) nanoparticles can be easily synthesized and incorporated into polymeric matrices, making it possible to use them as additives against bacterial action. The antibacterial activity of silver nanoparticles relies on several mechanisms, including damage to the cell wall, increase in the permeability and leakage of intracellular substances, alteration in the expression of envelope proteins and heat shock proteins, dissipation of the proton motive force, collapse of the plasma membrane potential, and decrease of intracellular ATP [3, 4]. Additionally, the liberation of silver ions increases the

bactericidal effect since they are known to participate in the generation of reactive oxygen species, alter proteins by interacting with thiol groups, and induce DNA condensation leading to the loss of bacterial replication [5, 6].

On the other hand, titanium dioxide (TiO_2) is an additive currently used in the plastic industry that can also exhibit photocatalytic properties when it is exposed to UV radiation leading to the generation of electrons and holes that are able to oxidize water and hydroxide ions to produce highly reactive hydroxyl radicals capable of decomposing bacterial cell membranes [7]. These properties of TiO_2 can also be enhanced by the presence of silver nanoparticles on its surface (Ag/TiO_2). For instance, photocatalytic degradation of rhodamine B and 2,4,6-trichlorophenol was more effective using Ag/TiO_2 than TiO_2 alone, and TiO_2 films that contained silver exhibited a higher antibacterial activity against *Escherichia coli* than TiO_2 by itself [8–10]. The use of Ag/TiO_2 nanoparticles is presented in this work as a potential antibacterial additive given the properties of the individual components. They were obtained by simultaneous synthesis and deposition of Ag nanoparticles on the TiO_2 particle surface through a deposition-precipitation method, which allows for a controlled particle growth [11]. The materials generated by this method present higher photo oxidizing activities than those synthesized using other procedures (colloidal deposition, photodeposition, impregnation, etc.) [12, 13]. However, the size, shape, and metal concentration on the surface of the support are sensitive to parameters such as the pH of the reaction mixture [14–16]. For that reason, in this study we have synthesized Ag/TiO_2 varying the pH and keeping constant all other synthesis conditions. We have found that while nanoparticle size is not affected by pH variations, the presence of Ag on the TiO_2 surface is sensitive to this difference, being greater at pH 9. Ag/TiO_2 nanoparticles were then incorporated into PS through an extrusion-injection process, resulting in rectangular pieces containing 100, 300, 500, and 700 ppm (wt.) of Ag/TiO_2, with respect to the PS content. The PS containing this additive displays antibacterial properties against *Escherichia coli* even in the absence of light. As discussed, this property is directly related to the presence of the Ag/TiO_2 on the PS surface and also to the effectivity of the Ag in this additive.

2. Experimental

2.1. Silver Nanoparticles Synthesis and Deposition on TiO_2.
Ag/TiO_2 nanoparticles were synthesized in the absence of light through a deposition-precipitation method using silver nitrate (Fermont) as metallic precursor, sodium hydroxide (Caledon Laboratories LTD) as reducing agent, and TiO_2 Degussa P25 (Degussa Corporation/Pigments Group) as support. Briefly, an aqueous solution of silver nitrate containing 1.5 wt.% of silver on TiO_2 was added to an aqueous suspension of TiO_2. The mixture was heated to 80°C under vigorous stirring and the pH was adjusted to 9, 11, or 12 using sodium hydroxide. Heating and mixing were held for two hours, then the solution was centrifuged (10000 rpm), and

the precipitate was washed with water at 50°C. After a second centrifugation, the solid was dried in an oven at 80°C for 12 hours, ground, and stored in the dark.

2.2. Nanoparticle Characterization.
The size and shape of Ag/TiO_2 particles were characterized by a JEOL JEM-1230 TEM operated at 100 KV in the bright field imaging mode. Particle size and size distributions were calculated by measuring around 200 metal particles. SEM-EDX analysis was performed on a Philips FEI microscope model XL-30-PW6630/01 operated at 20 kW.

2.3. Extrusion of Polystyrene with Ag/TiO_2.
A mixture of Ag/TiO_2 and PS was injected using an Injection Molding Machine Battenfeld, Model LCMI in which the temperature of the barrel ranged between 190 and 210°C. The temperature of the mold was 27°C, the shoot volume was 43 cc, the screw speed was of 43 rpm, the pressure was 8.27 MPa, the cooling time was 15 s, and the cycle consisted of 31 s in total. This process resulted in the production of PS-Ag/TiO_2 rectangular pieces with dimensions of $100 \times 70 \times 3$ mm, which contained 100, 300, 500, and 700 ppm (wt.) of Ag/TiO_2 with respect to the PS content.

2.4. Polystyrene-Ag/TiO_2 Surface Characterization.
An Atomic Force Microscope (AFM) Multimode with a Nano-Scope IIIa controller (Veeco Metrology Group, Santa Barbara, USA) was used in intermittent contact mode using nonconductive silicon rectangular cantilevers (Bruker MPP-11120, tip radius ~8 nm) with a length of 125 μm and nominal frequency of 300 KHz to obtain images in phase contrast, which allowed the study of the dispersion of Ag/TiO_2 nanoparticles on the PS surface. The images were processed by using the NanoScope Analysis software (version 1.40, Bruker Corporation). The presence of the nanoparticles on the PS surface was confirmed by analyzing the phase histogram from the raw data matrix acquired. The percentage of the PS surface covered by Ag/TiO_2 was estimated as the ratio between the areas under the peaks observed in the phase distribution of the samples:

$$\% \text{ of PS surface covered} = \left(\frac{A_{\text{NP}}}{A_{\text{PS}} + A_{\text{NP}}} \right) 100, \quad (1)$$

where the subindexes PS and NP refer to the PS surface and the nanoparticles, respectively. Additionally, the dissipated energy during the tip-surface interaction can be calculated from the change in the oscillation amplitude and phase lag ϕ, using the equation:

$$E_{\text{dis}} = \left(\sin \varphi - \frac{A}{A_0} \right) \frac{\pi k A A_0}{Q} \quad (2)$$

in which A is the amplitude during testing, A_0 is the free amplitude, k is the force constant of the cantilever, and Q is the quality factor [17]. This dissipative energy is used to distinguish different components on the material surface [18–20].

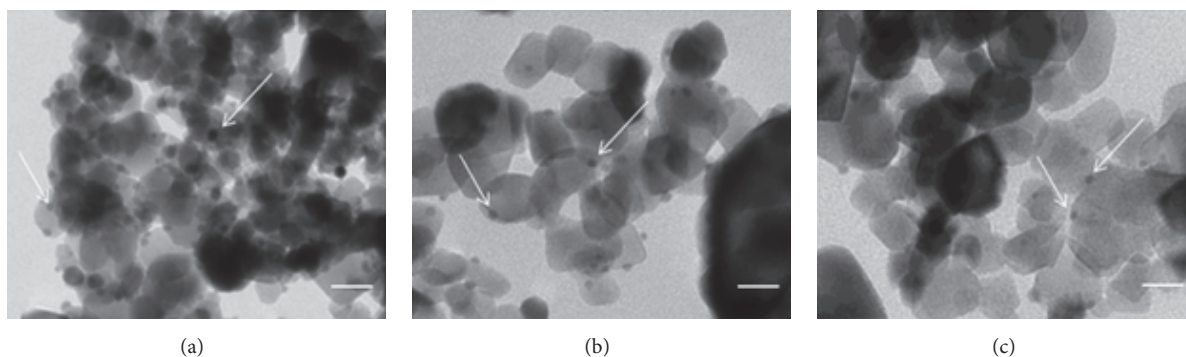(a)   (b)   (c)

FIGURE 1: TEM images of silver nanoparticles (arrows) deposited on TiO$_2$, synthesized at pH 9 (a), pH 11 (b), and pH 12 (c). At all the pH values showed, nanoparticles presented the same form with an average size ranging from 5.6 to 6.0 nm, while the average size of TiO$_2$ was 35 ± 10 nm. At pH 9, Ag nanoparticles were more abundant. The scale line represents 20 nm.

2.5. Antibacterial Activity of PS-Ag/TiO$_2$ Samples. Antibacterial tests, performed on *Escherichia coli* ATCC 25922, were conducted as follows: 400 μL of a bacterial suspension containing a total of 4×10^5 colony forming units was placed at the center of the test surface that had been previously cut to a square with dimensions of 50×50 mm. The suspension on the PS surface was covered using a flexible film square (40×40 mm) and the sample was incubated in a chamber (relative humidity > 90%), in the dark, at 35 ± 1°C for 24 ± 1 hours. It must be kept in mind that under this condition (incubation in the absence of light) it is unlikely that TiO$_2$ will exhibit antibacterial effect, since this is dependent on its photocatalytic properties. Therefore, antibacterial activity of the sample will only be attributed to the action of silver. After the incubation, the sample was placed on a plastic bag and 10 mL of Tryptic Soy Broth (Bioxon) was added and used to wash the sample in views to recover the bacteria present in it. The bacterial count was performed using the Pour Plate method: from the wash, dilutions ranging from 10^{-1} to 10^{-10} were made in Phosphate Buffer Saline and 1 mL of each dilution was placed in a petri dish to which liquid Plate Count Agar (Bioxon) was added. The sample was homogenized and after the agar hardened it was incubated at 35 ± 1°C for 48 hours. Counting was performed in plates containing between 30 and 300 colonies.

3. Results and Discussion

3.1. Characterization of Ag/TiO$_2$ Nanoparticles. The size of silver nanoparticles was obtained from the analysis of TEM images as presented in Figure 1. The silver nanoparticles synthesized at pH of 9, 11, and 12, using 1.5 wt.% of Ag/TiO$_2$, are presented in Figures 1(a), 1(b), and 1(c), respectively. The average Ag particle sizes obtained were 5.7 ± 1.6 nm, 6.0 ± 1.9 nm, and 5.6 ± 1.4 nm, respectively. All nanoparticles displayed approximately the same shape regardless of the pH, even though the influence of pH on nanoparticle assembly, size, and distribution was previously reported [21–23]; in our case for the different pH evaluated, it did not seem to have a determining effect on the particle size. The effect of

metal loading of Ag on TiO$_2$ as confirmed by SEM-EDX analysis and scanning electron micrography is presented in Figure 2(a) where the following can be observed the presence of agglomerates of Ag/TiO$_2$ composites on the surface of the polymer and in Figure 2(b) the EDS analysis to determine metal loadings, showing that the effect of pH did not have a significant effect on the amount of silver deposited: 1.28 ± 0.3, 1.40 ± 0.34, and 1.37 ± 0.21 wt.%, respectively, for pH 9, pH 11, and pH 12.

3.2. AFM Characterization of PS-Ag/TiO$_2$ Samples. Figure 3 presents AFM height, phase contrast, and energy dissipation images (columns (a), (b), and (c), resp.) of a PS matrix containing 100, 300, 500, and 700 ppm of Ag/TiO$_2$, acquired within the month of its fabrication. These images showed distinctive local zones produced by the presence of nanoparticles at the surface of the material which contrasts with the reference sample that consists of pure PS. The presence of the nanoparticles on the PS surface is expected due to their difference in solubility: while PS is hydrophobic in nature and nanoparticles are hydrophilic, this difference induces the presence of Ag/TiO$_2$ on the PS surface. In addition, the temperatures used for the injection of PS and Ag/TiO$_2$ could facilitate the migration of the particles into the surface [24].

Figure 3 also highlights that the presence of agglomerates of the antibacterial additive reaches a maximum at a concentration of 700 ppm. This last result is not surprising since nanoparticles tend to agglomerate due to the large interparticle forces that exist between them (i.e., van der Waals forces) [25, 26].

The dispersion of these nanoparticles on the PS surface is corroborated by the analysis of the phase histograms shown in Figure 4. As observed, there are three histograms with a bimodal distribution (at 100, 300, and 700 ppm) and two with a unimodal distribution (at 0 and 500 ppm). The existence of two modes exhibits a poor distribution of the additive into the matrix surface, while the unimodal distribution coincides with the image from the PS alone and the image from the sample with the best nanoparticle distribution on the surface. In consequence, the nanoparticle dispersion on the PS surface was favored at low concentrations of Ag/TiO$_2$,
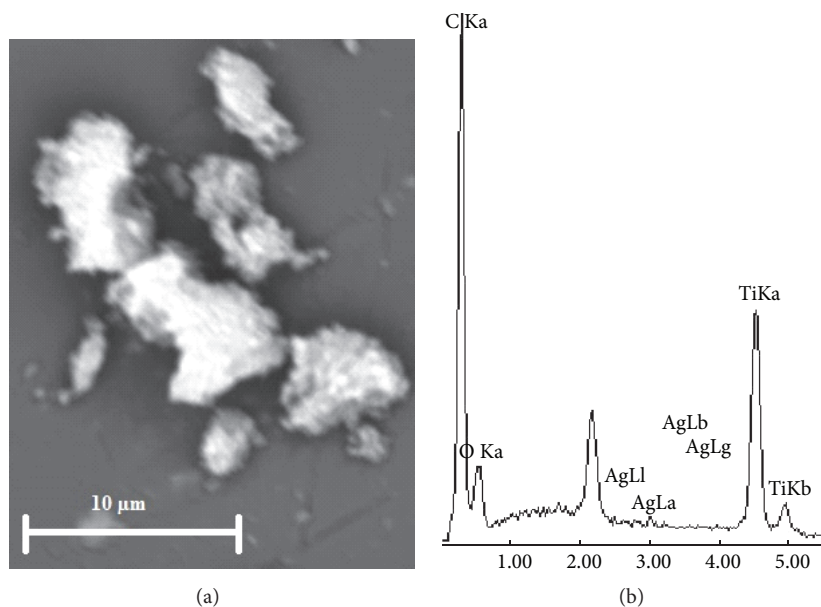
FIGURE 2: (a) SEM image of Ag/TiO$_2$ composite on polystyrene; (b) EDX spectrum of Ag/TiO$_2$ composites.

with the most homogenous distribution of nanoparticles achieved at 500 ppm. In order to confirm the presence of the nanoparticles on the PS surface, the energy dissipation of the cantilever's oscillation was calculated, to give the energy that we are losing each cycle of the tapping mode as that value will depend on the material, resulting in values between 29.2 and 44.0 aJ for the PS, in accordance with previous reports, and values between 8.8 and 21.4 aJ for the regions affected by the nanoparticles [20]. This reduction in energy is expected for the nanoparticles given that they dissipate less energy and therefore indicate the dispersion of a harder additive (Ag/TiO$_2$) into the surface of a softer (PS) matrix. This approach presents a nondestructive subsuperficial characterization technique that avoids heating, radiolysis, and degradation of the polymer matrix.

The percentage of surface coverage of the PS samples containing different amounts of Ag/TiO$_2$ was calculated from results presented in Figure 5, as described above. The values obtained were 54.7%, 52.3%, 89.3%, and 23.1% for the samples containing 100, 300, 500, and 700 ppm. These values, related to the surface coverage, are a clear indicator of the expected antibacterial effects of these composites.

3.3. Antibacterial Activity of PS-Ag/TiO$_2$ Samples. Antibacterial activity was evaluated through the inoculation of 4×10^5 colony forming units of *E. coli* on the different PS plates containing Ag/TiO$_2$. The inoculation was followed by a 24 ± 1 hours of incubation. As shown in Figure 4, PS-Ag/TiO$_2$ pieces display different degrees of antibacterial activity compared to bare PS and said activity is directly related to the surface coverage of the PS samples with Ag/TiO$_2$. It is important to note that the PS test pieces inhibited bacterial growth by more than 80% at Ag/TiO$_2$ loadings of 100 ppm, 300 ppm, and 500 ppm. The antibacterial activity of Ag/TiO$_2$ nanoparticles on PS could be the result of one or several of the antibacterial

mechanisms mentioned above (see Section 1). On the other hand, a severe decrease in the antibacterial activity was observed for Ag/TiO$_2$ 700 ppm, indicating that there is a concentration limit beyond which the antibacterial effect of this additive is diminished. This is evidently related to the Ag/TiO$_2$ agglomerates formed at 700 ppm, which reduce the contact surface between the antibacterial composite and *E. coli* resulting in less bacterial death than for the other concentrations in which the nanoparticles are more evenly distributed on the PS surface. Taking into consideration this information and the data obtained from the AFM images, it is evident that the antibacterial effect of Ag/TiO$_2$ is more likely a result of its distribution in the surface of the PS, rather than of its bulk concentration.

4. Conclusions

An antibacterial additive based on Ag/TiO$_2$ nanoparticles was evaluated and validated using PS as plastic matrix. Ag/TiO$_2$ nanoparticles were mixed with the PS through an extrusion-injection process and nanoparticles were localized on the PS surface, as shown by AFM characterization. Indeed, the antibacterial effect was directly correlated with the presence of the Ag/TiO$_2$ nanoparticles on the PS surface. The antibacterial tests against *E. coli* were carried at 100, 300, 500, and 700 ppm (wt) of Ag/TiO$_2$, with respect to the PS content, in the absence of light to assess the effect of Ag in the antibacterial additive. At low concentrations (100, 300, and 500 ppm), bacterial growth inhibition was greater than 80%, showing that Ag/TiO$_2$ has good antibacterial properties independently of the concentration values. However, agglomerates were observed at 700 ppm accompanied by a diminishing antibacterial effect. This finding established a limit for the additive concentration that can be used for the production of antibacterial PS surfaces. The previous
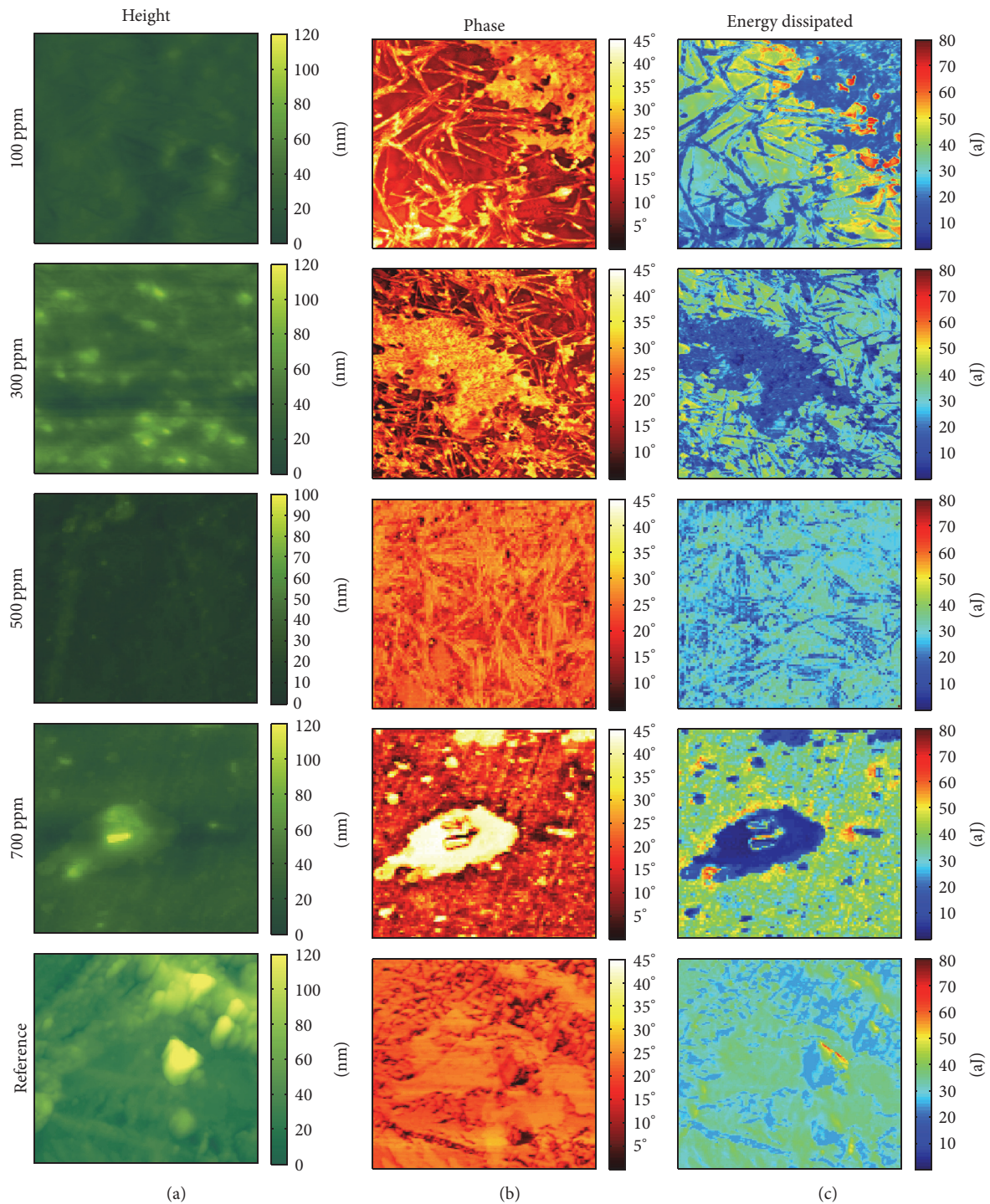
FIGURE 3: AFM height, phase contrast, and energy dissipation images of a PS matrix with different amounts of Ag/TiO$_2$ nanoparticles. Color contrast observed on the surfaces is related to the presence of Ag/TiO$_2$ nanoparticles on those regions. Some agglomerates are observed in the sample containing 700 ppm of Ag/TiO$_2$.

result shows a promising approach for the development of a new family of antimicrobial additives for plastics. There is undoubtedly a trend toward the use of more environmental friendly antimicrobials with low toxicity.Antimicrobials based on silver substances meet this favorable toxicity profile and can be used at relatively low concentrations on the surface of plastic, showing important advantages over agents that cannot make similar claims.
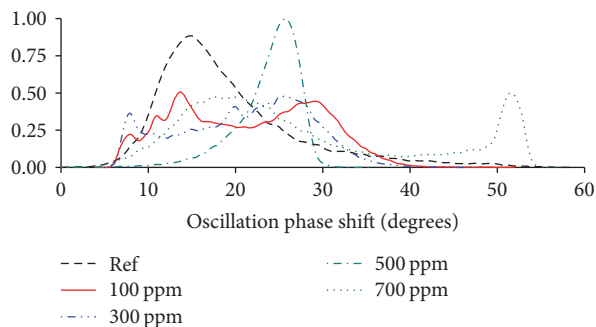
FIGURE 4: Phase histogram of PS sample containing Ag/TiO$_2$ nanoparticles. Wide, bimodal histogram is observed for 100, 300, and 700 ppm of Ag/TiO$_2$, showing the presence of PS and the additive. On the contrary, reference and the sample containing 500 ppm of Ag/TiO$_2$ produce a unimodal distribution indicating that the additive homogenously covers the PS surface.
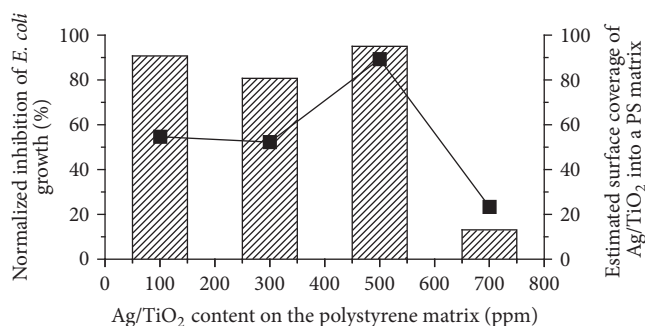

FIGURE 5: Antibacterial growth inhibition of polystyrene-based samples as Ag/TiO$_2$ concentration increases. Values are normalized with respect to a reference sample of pure polystyrene. Markers represent the estimated surface coverage of the Ag/TiO$_2$. The inhibition of E. coli growth is directly related to the surface coverage of Ag/TiO$_2$ on the PS surface.

Competing Interests

The authors declare that there is no conflict of interests regarding the publication of this paper.

Acknowledgments

References

[1] H. Zweifel, *Plastic Additives Handbook*, Hanser Gardner Publications, Munich, Germany, 2001.

[2] S. Ebnesajjad and K. Modjarrad, *Handbook of Polymer Applications in Medicine and Medical Devices*, Elsevier, 2013.

[3] I. Sondi and B. Salopek-Sondi, "Silver nanoparticles as antimicrobial agent: a case study on *E. coli* as a model for Gram-negative bacteria," *Journal of Colloid and Interface Science*, vol. 275, no. 1, pp. 177–182, 2004.

[4] C.-N. Lok, C.-M. Ho, R. Chen et al., "Proteomic analysis of the mode of antibacterial action of silver nanoparticles," *Journal of Proteome Research*, vol. 5, no. 4, pp. 916–924, 2006.

[5] H.-J. Park, J. Y. Kim, J. Kim et al., "Silver-ion-mediated reactive oxygen species generation affecting bactericidal activity," *Water Research*, vol. 43, no. 4, pp. 1027–1032, 2009.

[6] Q. L. Feng, J. Wu, G. Q. Chen, F. Z. Cui, T. N. Kim, and J. O. Kim, "A mechanistic study of the antibacterial effect of silver ions on *Escherichia coli* and *Staphylococcus aureus*," *Journal of Biomedical Materials Research*, vol. 52, no. 4, pp. 662–668, 2000.

[7] S.-Q. Sun, B. Sun, W. Zhang, and D. Wang, "Preparation and antibacterial activity of Ag-TiO$_2$ composite film by liquid phase deposition (LPD) method," *Bulletin of Materials Science*, vol. 31, no. 1, pp. 61–66, 2008.

[8] H. M. Sung-Suh, J. R. Choi, H. J. Hah, S. M. Koo, and Y. C. Bae, "Comparison of Ag deposition effects on the photocatalytic activity of nanoparticulate TiO$_2$ under visible and UV light irradiation," *Journal of Photochemistry and Photobiology A: Chemistry*, vol. 163, no. 1-2, pp. 37–44, 2004.

[9] S. Rengaraj and X. Z. Li, "Enhanced photocatalytic activity of TiO$_2$ by doping with Ag for degradation of 2,4,6-trichlorophenol in aqueous suspension," *Journal of Molecular Catalysis A: Chemical*, vol. 243, no. 1, pp. 60–67, 2006.

[10] O. Akhavan, "Lasting antibacterial activities of Ag-TiO$_2$/Ag/a-TiO$_2$ nanocomposite thin film photocatalysts under solar light irradiation," *Journal of Colloid and Interface Science*, vol. 336, no. 1, pp. 117–124, 2009.

[11] Z. V. Quiñones-Jurado, M. Á. Waldo-Mendoza, H. M. Aguilera-Bandin, E. G. Villabona-Leal, E. Cervantes-González, and E. Pérez, "Silver nanoparticles supported on TiO$_2$ and their antibacterial properties: effect of surface confinement and nonexistence of plasmon resonance," *Materials Sciences and Applications*, vol. 5, no. 12, pp. 895–903, 2014.

[12] L. Prati and A. Villa, "The art of manufacturing gold catalysts," *Catalysts*, vol. 2, no. 1, pp. 24–37, 2011.

[13] S. Oros-Ruiz, J. A. Pedraza-Avella, C. Guzmán et al., "Effect of gold particle size and deposition method on the photodegradation of 4-chlorophenol by Au/TiO$_2$," *Topics in Catalysis*, vol. 54, no. 8-9, pp. 519–526, 2011.

[14] M. Haruta, "Size- and support-dependency in the catalysis of gold," *Catalysis Today*, vol. 36, no. 1, pp. 153–166, 1997.

[15] R. Zanella, S. Giorgio, C. R. Henry, and C. Louis, "Alternative methods for the preparation of gold nanoparticles supported on TiO$_2$," *Journal of Physical Chemistry B*, vol. 106, no. 31, pp. 7634–7642, 2002.

[16] K. R. Souza, A. F. F. de Lima, F. F. de Sousa, and L. G. Appel, "Preparing Au/ZnO by precipitation–deposition technique," *Applied Catalysis A: General*, vol. 340, no. 1, pp. 133–139, 2008.

[17] N. F. Martínez and R. García, "Measuring phase shifts and energy dissipation with amplitude modulation atomic force microscopy," *Nanotechnology*, vol. 17, no. 7, pp. S167–S172, 2006.

[18] R. Garcia, C. J. Gómez, N. F. Martinez, S. Patil, C. Dietz, and R. Magerle, "Identification of nanoscale dissipation processes by dynamic atomic force microscopy," *Physical Review Letters*, vol. 97, no. 1, Article ID 016103, 2006.

[19] Y. H. Liu, D. Wang, K. Nakajima et al., "Characterization of nanoscale mechanical heterogeneity in a metallic glass by dynamic force microscopy," *Physical Review Letters*, vol. 106, no. 12, Article ID 125504, 2011.

[20] D. Wang, X.-B. Liang, Y.-H. Liu, S. Fujinami, T. Nishi, and K. Nakajima, "Characterization of surface viscoelasticity and energy dissipation in a polymer film by atomic force microscopy," *Macromolecules*, vol. 44, no. 21, pp. 8693–8697, 2011.

[21] P. K. Sahoo, S. S. Kalyan Kamal, T. J. Kumar, B. Sreedhar, A. K. Singh, and S. K. Srivastava, "Synthesis of silver nanoparticles using facile wet chemical route," *Defence Science Journal*, vol. 59, no. 4, pp. 447–455, 2009.

[22] M. Kamali, S. A. A. Ghorashi, and M. A. Asadollahi, "Controllable synthesis of silver nanoparticles using citrate as complexing agent: characterization of nanoparticles and effect of pH on size and cristallinity," *Iranian Journal of Chemistry and Chemical Engineering*, vol. 31, pp. 21–28, 2012.

[23] M. Vanaja, S. Rajeshkumar, K. Paulkumar, G. Gnanajobitha, C. Malarkodi, and G. Annadurai, "Kinetic study on green synthesis of silver nanoparticles using *Coleus aromaticus* leaf extract," *Advances in Applied Science Research*, vol. 4, pp. 50–55, 2013.

[24] X. Xu, Z. Zhang, and W. Liu, "Fabrication of superhydrophobic surfaces with perfluorooctanoic acid modified TiO_2/ polystyrene nanocomposites coating," *Colloids and Surfaces A: Physicochemical and Engineering Aspects*, vol. 341, no. 1–3, pp. 21–26, 2009.

[25] T. P. Selvin, J. Kuruvilla, and T. Sabu, "Mechanical properties of titanium dioxide-filled polystyrene microcomposites," *Materials Letters*, vol. 58, no. 3-4, pp. 281–289, 2004.

[26] A. Chandra, L.-S. Turng, S. Gong, D. C. Hall, D. F. Caulfield, and H. Yang, "Study of polystyrene/titanium dioxide nanocomposites via melt compounding for optical applications," *Polymer Composites*, vol. 28, no. 2, pp. 241–250, 2007.